International Journal of Fracture **106**: L9-L14, 2000.

SOME REMARKS ON HYDROGEN TRAPPING

Tarek I. Zohdi
Institute for Structural Mechanics and Computational Mechanics
Appelstrasse 9A, 30167 Hannover, Germany
zohdi@ibnm.uni-hannover.de fax. 49-(0511)-762-5496

Abstract. A model for the pressure-dependent diffusion and accumulation of hydrogen ahead of a decohesive intergranular crack front is developed. In the model, the pressure dependency of the diffusion is incorporated into the activation energy of an Arrhenius form of the material diffusivity along high-diffusivity grain boundaries. A key feature of the model is the ability to describe the trapping of hydrogen ahead of a decohesive crack front, which is observed in laboratory experiments.

1. Introduction. In many cases subcritical intergranular crack growth, so-called granular decohesion, can be directly traced to the presence of hydrogen at grain boundaries (see for example Gerberich et. al. [1]). In Zohdi and Meletis [2] discontinuous hydrogen-assisted mode-I intergranular cracking was observed in rolled AL-2.2Li-2.9Cu-0.12Zr aluminum-lithium alloy in the T8 condition. The term *discontinuous* denotes that the crack front propagates, then arrests, with the process then repeating itself. In other words, *the decohesive front grows discontinuously with time.* In the experiments mentioned, the length of the individual jumps corresponded quite well to the (plastic) process zone size directly ahead of the crack. These jumps were located by determining crack arrest marking with a scanning electron microscope. The experimental results suggest that a buildup of hydrogen must occur directly ahead of the crack front. This is consistent with observations of other authors. See for example Doig and Jones [3], Unger and Aifantis [4], [5], Sofronis and McMeeking [6], Lufrano and Sofronis [7] and Lufrano, et. al. [8], [9] for details. The goal of this communication is to develop a relatively simple model to describe hydrogen trapping ahead of an intergranular crack tip.

2. Pressure-dependent activation energy. We start by constructing a quasi-Fickian diffusion model describing the diffusion of a small solute in a stressed solid. The stress-dependency is embedded in the activation energy of an Arrhenius law, $\boldsymbol{G} = -\mathbb{D}_0 e^{\frac{-U(\boldsymbol{\sigma})}{R\theta}} \cdot \nabla c$, where c is the normalized concentration of the solute (molecules per unit volume), $\boldsymbol{G}$ is the flux of the small solute, measured by hydrogen molecules per unit area per unit time, $\mathbb{D}_0$ is the diffusivity tensor (area per unit time) at a reference temperature, U is the activation energy for solute motion (per mole of diffusive species), $\boldsymbol{\sigma}$ is the Cauchy stress, and R is the universal gas constant. We assume an

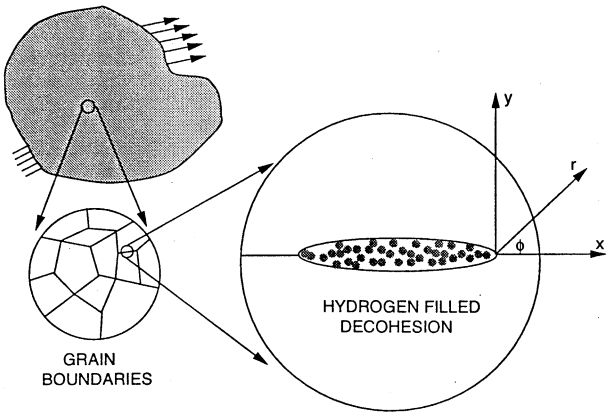

Figure 1: An idealization of an intergranular hydrogen-filled decohesive front.

additive spilt of the activation energy, $U(\boldsymbol{\sigma}) = U_0 + \tilde{U}(P)$, where U_0 is a stress-independent reference activation energy and $P = -\frac{tr\boldsymbol{\sigma}}{3}$ is the pressure. From physical reasoning, it is logical to assume that for $P < 0$, $\tilde{U}(P) < 0$, for $P > 0$, $\tilde{U}(P) \geq 0$, and for $P = 0$, $\tilde{U}(P) = 0$. If we expand $\tilde{U}(P)$ around $P = 0$ we obtain $\tilde{U}(P) = 0 + \frac{\partial \tilde{U}(P)}{\partial P}|_{P=0} P + ... = \eta P$, $\eta \geq 0$. The end effect is that the solid attains an "apparent" heterogeneous diffusive composition, $\mathbb{D}_0 e^{\frac{-(U_0+\eta P)}{R\theta}}$, of relatively high diffusivity in negative pressure regions and relatively low diffusivity in positive pressure regions.

To model the pressure fields ahead of the decohesive front, we consider an initially sharp mode-I crack, producing a singular linearly-elastic stress field, where $\sigma_{ij} = \frac{K_I}{\sqrt{2\pi r}} f_{ij}(\phi)$ and where the f_{ij} are functions of ϕ (Figure 1). Using standard notation, the stress intensity factor is $K_I = \zeta \sigma \sqrt{a}$, where a is half the length of the crack and where σ is the remote stress. For an infinite planar domain under remote uniaxial loading we have $\zeta = \sqrt{\pi}$. Throughout the analysis we consider only plane strain conditions. Correspondingly, we have for the pressure

$$P(r,\phi) = -\frac{2(1+\nu)}{3} \frac{K_I}{\sqrt{2\pi r}} cos\frac{\phi}{2}, \tag{1}$$

where ν is the material Poisson ratio. At the crack tip, the pressure is singular ($P = \mathcal{O}(r^{-\frac{1}{2}})$), and thus when inserted into the Arrhenius law, the diffusivity also becomes singular. As a form of regularization, we consider material plastification ahead of the crack and that the crack tip blunts. To approximate the pressure fields ahead of the crack, we must first approximate the plastic zone. This is done by computing the domain within an envelope of points where the

von Mises criteria holds, i.e. $\boldsymbol{\sigma}' : \boldsymbol{\sigma}' = \frac{2\mathcal{Y}}{3}$, where $\boldsymbol{\sigma}'$ is the deviatoric stress, and $\mathcal{Y}$ is the yield stress obtained from a uniaxial tension test. Under plane strain conditions, this leads to a radial envelope function of the plastic zone given by

$$r_p(\phi) = \frac{K_I^2}{4\pi\mathcal{Y}^2}\left(\frac{3}{2}sin^2\phi + (1-2\nu)^2(1+cos\phi)\right). \tag{2}$$

Since the diffusion along grain boundaries is approximately 1000 times greater than in the transgranular direction, the diffusion process is considered one dimensional. Therefore, a specific plane, that of $\phi = 0$, i.e along the grain boundary, is of primary interest. Assuming perfect plasticity and no work hardening, we can use the classical slip-line solution of Hill [10] for a notched bar in tension, to arrive at the following expression for the pressure (Figure 2)

$$P(x) = -\mathcal{Y}\left(Ln(1+\frac{x}{\rho}) + \frac{1}{2}\right), \tag{3}$$

where x is the distance ahead of the crack tip and where ρ is the crack tip radius. This field is used in the plastic zone, while the elastic field is used in the remainder of the body. This approximation neglects the redistribution of the stress field in the elastic portion of the body, and thus is a good approximation only when the plastic zone size is small compared to other length scales in the problem. This is assumed to be the case in the present study. In corrosion literature, this is a frequently used model, for example see works dating back to Doig and Jones [3]. Clearly, the stress fields ahead of a blunted crack could be computed by finite element methods, for example see McMeeking [11] and Sofronis and McMeeking [6]. However, in this work we continue to use the slip-line solution, which is adequate for the scope of this work. Knowing that along the $\phi = 0$ line the pressure must be equal at the elastic plastic interface, i.e. at $x = r_p$, allows us to equate the pressure expressions in Equations 1 and 3 to solve for the crack tip radius ρ

$$. \ \rho = \frac{r_p}{e^{\left(\frac{2}{3}\frac{(1+\nu)}{(1-2\nu)} - \frac{1}{2}\right)} - 1}. \tag{4}$$

3. Qualitative and quantitative behavior. In order to extract some information on the qualitative behavior of the model, we first consider a two point boundary value problem describing *steady state* diffusive solution behavior along a grain boundary. Accordingly, consider a ligament ahead of a blunted mode-I crack (Figure 2) to form the following two point boundary value problem: $\nabla \cdot (\boldsymbol{I\!D}_0 e^{\frac{-U(\sigma)}{R\theta}} \cdot \nabla c) = \dot{c} = 0$, $c(x=0,t) = c_s = 1$ and $c(x=L,t) = 0$

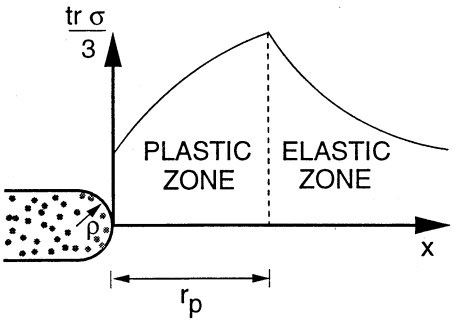

Figure 2: A blunted crack, and the corresponding elaso-plastic hydrostatic stress field.

($r_p << L$), where the concentrations have been normalized for convenience. The solution is monotonically decreasing, starting from the front surface

$$c(x) = c_s + M \int_0^x \frac{1}{D_0 e^{-(\frac{U_0+\eta P}{R\theta})}} dx, \text{ where } M = -\frac{c_s}{\int_0^L \frac{1}{D_0 e^{-(\frac{U_0+\eta P}{R\theta})}} dx}. \quad (5)$$

Since the term $D_0 e^{-\frac{(U_0+\eta P)}{R\theta}}$ is relatively large in the plastic zone, the concentration stays relatively high in that region. However, once $D_0 e^{-(\frac{U_0+\eta P}{R\theta})}$ starts to drop, the concentration decreases more rapidly. Essentially, since the pressure (which is negative) grows rapidly, a "flux-barrier" is formed that permits only limited solute penetration, i.e. low concentration gradients and low fluxes. The nonmonotone elasto-plastic pressure field ahead of the crack will lead high solute accumulation, since the homogeneous diffusivity (D_0) is transformed into a spatially heterogeneous one ($D_0 e^{\frac{-(U_0+\eta P)}{R\theta}}$).

Consider a quantitative example where the material values used are taken from experiments in Zohdi and Meletis [2] for AL-2.2Li-2.9Cu-0.12Zr aluminum-lithium alloy in the T8 condition. The values are as follows: $\nu = 0.295$, $\mathcal{Y} = 307$ (MPa), $K_I = 8.62\, MPam^{\frac{1}{2}}$. The selected mechanical parameters led to a computed plastic zone size of $r_p = 21\ \mu m$, whereas the experimental values were approximately between 20 and 30 μm. The computed value for the crack tip radius was $\rho = 5.3\ \mu m$. We defined a critical value for the pressure dependency parameter (η), which would force $U = U_0 + \tilde{U}(P) = 0$ at the plastic-elastic interface, $\eta^* \stackrel{\text{def}}{=} -\frac{U_0}{P(r_p)}$. The experimental value of $U_0 = 7000$ ($\frac{Nm}{mole}$) for the activation energy was used. For the selected material values, $\eta^* = 1.059 \times 10^{-5} \frac{m^3}{mole}$. Various values of η, normalized with respect to η^*,

were used, i.e. $\eta = \gamma\eta^*$, $0 \leq \gamma \leq 1$. The results are shown in Figures 3 and 4. The concentration gradient is $\frac{dc(x)}{dx} = \frac{M}{D_0} e^{(\frac{U_0+\eta P}{R\theta})}$, thus one observes that the term controlling the concentration gradient is $e^{\frac{(U_0+\eta P)}{R\theta}}$ drops rapidly, thus locally trapping the hydrogen. One can interpret the stress state as producing a relatively high effective diffusivity immediately ahead of the crack. Further ahead, the effective diffusivity then decreases rapidly. The combined effects cause accumulation of hydrogen in the plastic zone.

4. Concluding remarks. The model presented can be incorporated into time transient decohesive hydrogen front propagation simulations rather easily. For specific materials such simulations are being currently pursued by the author.

REFERENCES

1. Gerberich, W.W., Livne, T., Chen, X. F., Kaczorowski, M. (1988). Crack growth from hydrogen-temperature and microstructural effects in 4340 steel. Metall. Trans. 19A, 1319-1334.
2. Zohdi, T. I. and Meletis, E. I. (1992). On the intergranular hydrogen embrittlement mechanism of Al-Li alloys. Scripta Metallurgica. **26**, 1615-1620.
3. Doig, P. and Jones, T.(1977) A model for the initiation of hydrogen embrittlement cracking at notches in gaseous hydrogen environments. Metall. Trans. **18A**, 1993-1998.
4. Unger, D. J. and Aifantis, D. C. (1983) On the theory of stress-assisted diffusion, II. Acta Mechanica. **47**, 117-151
5. Unger, D. J., Gerberich, W. W. and Aifantis, D. C. (1982) Further remarks on the implications of steady-state stress-assisted diffusion on environmental cracking. Scripta Metallurgica. **16**, 1059-1064
6. Sofronis, P. and McMeeking, R. M. (1989). Numerical analysis of hydrogen transport near a blunting crack tip. J. Mech. Phys. Solids **37**, 317-350.
7. Lufrano, J. and Sofronis, P. (1996). Numerical analysis of the interaction of solute hydrogen atoms with the stress field of a crack. Int. J. Solids Structures **33**, No. 12. 1709-1723.
8. Lufrano, J., Sofronis, P. and Birnbaum, H. K. (1996). Modeling of hydrogen transport and elastically accommodated hydride formation near a crack tip. J. Mech. Phys. Solids. **44**, 179-205.
9. Lufrano, J., Sofronis, P. and Birnbaum, H. K. (1998). Elastoplastically accommodated hydride formation and embrittlement. J. Mech. Phys. Solids. **46** No. 9, 1497-1520.
10. Hill, R. (1950). The mathematical theory of plasticity. Clarendon Press.
11. McMeeking, R. M. (1977). Finite deformation analysis of crack tip opening in elastic-plastic materials and implications for fracture. J. Mech. Phys. Solids. **25**, 357-381.

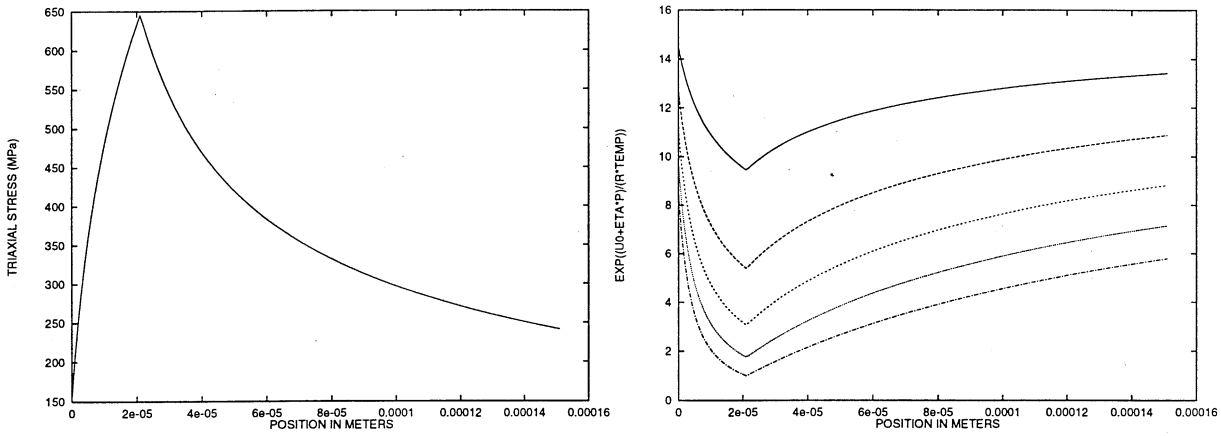

Figure 3: The hydrostatic stress field used to generate the effective diffusivities. The behavior of $e^{\frac{(U_0+\eta P)}{R\theta}}$ along the intergranular zone for various values of η: $\eta_1 = 0.2\eta^*$, $\eta_2 = 0.4\eta^*$, $\eta_3 = 0.6\eta^*$, $\eta_4 = 0.8\eta^*$ and $\eta_5 = 1.0\eta^*$.

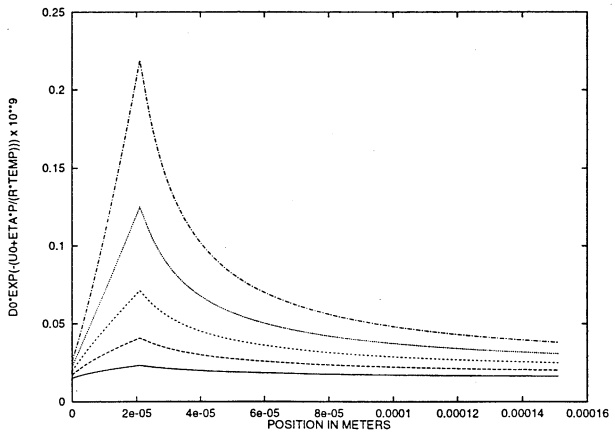

Figure 4: The behavior of $D_0 e^{-\frac{(U_0+\eta P)}{R\theta}}$ along the intergranular zone for various values of η: $\eta_1 = 0.2\eta^*$, $\eta_2 = 0.4\eta^*$, $\eta_3 = 0.6\eta^*$, $\eta_4 = 0.8\eta^*$ and $\eta_5 = 1.0\eta^*$.